Nonlinear Dynamic Analysis of Electrostatically Actuated Single-walled Carbon Nanotubes Using Nonlocal Elasticity

Abstract

The paper investigates the effects of application of nonlocal elasticity theory on electromechanical behaviors of single-walled carbon nanotubes under electrostatic actuation. The influences of different dimensions and boundary conditions on the vibration and dynamic instability of the carbon nanotubes are studied, in detail, using this theory. The results reveal that application of the nonlocal elasticity theory leads to the higher pull-in voltages for the nonlocal model applied for carbon nanotubes. Thus, in order to have more accurate results, one should apply nonclassical theorems such as the nonlocal elasticity theory to scrutinize the mechanical and electromechanical behaviors of the nano structures.

Keywords

Nonlinear dynamics, Carbon nanotubes, Nonlocal elasticity.

Mir M. Seyyed Fakhrabadi* [a]
Abbas Rastgoo [b]
Mohammad Taghi Ahmadian [c]

[a] School of Mechanical Engineering, College of Engineering, University of Tehran, Tehran, Iran
E-mail: msfakhrabadi@gmail.com
mfakhrabadi@ut.ac.ir
* Corresponding author
[b] School of Mechanical Engineering, College of Engineering, University of Tehran, Tehran, Iran
E-mail: arastgo@ut.ac.ir
[c] Department of Mechanical Engineering, Sharif University of Technology, Tehran, Iran
E-mail: ahmadian@sharif.edu

1 INTRODUCTION

Micro and nano electromechanical systems (MEMS/NEMS) have shown tremendous growth in both experimental and theoretical aspects during recent years; Sedighi et al. (2013), Kananipour et al. (2013). They are generally micro and nano structures such as micro/nano plates, shells, beams, wires and tubes sensed or actuated using some electrical mechanisms including piezoelectric, electro-

static and electrothermal techniques. The systems can be directly applied in the electronic circuits as micro/nano switches, capacitors, resonators, random access memories, etc. Thus, they have numerous real and potential applications in electronic, communication technology, aviation and automotive industries, etc. Hence, precise investigation of the mechanical and electromechanical behavior of the MEMS and NEMS is nowadays mandatory. Due to the high cost and current limitations in the fabrication processes of the micro and nano systems, experts make attempt to estimate the desired behaviors of the MEMS and NEMS using numerical modeling. For this purpose, researchers have tried to develop some novel models and techniques to obtain accurate results to agree well with the prototypes. This is more important for the NEMS due to the higher cost and more strict limitations in the related fabrication processes. Therefore, some researchers adopted the classical elasticity theories (CETs) and adapted them for nano scales to study the different mechanical behaviors of the nano systems; Kiani et al. (2013), Yang and Lim (2012).

Nano materials and nano structures can be categorized in different forms based on their materials, shapes, conductivities, etc. Some of them are metallic such as the nano particles fabricated from gold, silver and iron and rest of them are nonmetallic such as carbon-based nanomaterials. Obviously, their characteristics vary with respect to their substances. Carbon nanotube (CNT) as one the most applicable carbon-based nano structures possesses extraordinary physical, chemical, mechanical and electrical properties. It was discovered by Iijima (1991) and many scientists have scrutinized its different characteristics after the discovery; Fakhrabadi et al. (2012a), Fakhrabadi et al. (2012b), Chowdhury et al. (2009), Scarpa and Adhikari (2008). Many applications have been proposed for the CNTs ranging from nano medicine to nano engineering but one of the main utilizations considered for them is in NEMS. The CNTs are really well-fitted options for this field due to their strong mechanical structures, chemical stability and very high electrical conductivity, Koochi et al. (2014).

The deflection of the CNTs under electrostatic actuation and vdW forces was first studied by Dequesnes et al. (2002). They applied a one-degree-of-freedom model in their research which was a simplification and might have some deviation from the real system. They investigated the static behaviors of the CNTs under electrostatic actuation using the simplified single degree-of-freedom model. But, in this study, we will analyze the dynamic behavior of the mentioned nanosystem using continuum modeling and nonlocal elasticity theory to capture the size effects. In another research, Ke and Espinosa (2005) and Ke et al. (2005) developed studies of Dequesnes et al. (2012) via presenting two papers regarding the CNT-based NEMS. The first paper focused on the quality of charge distribution and the second one was about the stretching effects on the doubly clamped CNTs. In addition, Ouakad and Younis (2010) studied the dynamic behaviors of the CNTs under electrostatic actuation and presented the frequency response of the systems vs. different applied voltages.

Rasekh and Khadem (2010) completed the researches conducted in the field of mathematical formulation of the CNT-based NEMS via more comprehensive results about static and dynamic behaviors of the CNTs under electrostatic and vdW forces. They (2011) also investigated the effects of nonlinearity in curvature and inertia on the pull-in behaviors of the CNTs.
The main fact regarding the studies conducted on the mechanical and electromechanical behaviors of the nano systems and nano structures is their size-dependant properties. Some experiments revealed that the CETs often fail in predicting the mechanical properties of the micro and nano struc-

tures such as their natural frequencies and buckling loads, etc. Thus, scientists developed some novel theories to compensate this shortage in the continuum modeling of the micro/nano structures. One of the effective theorems is the nonlocal elasticity theory (NLET) developed by Eringen and Edelen (1972). According to this theory, the stress at a reference point x in an elastic body not only is a function of the strain at that point but also relates to the strain of the whole volume of the body, Arash and Wang (2012). This theory has been applied in various papers in order to obtain different models. For example, Wang and Liew (2007) applied the nonlocal continuum mechanics to study the static characteristics of the micro and nano structures. They analyzed the scale effects on the static deformation of the micro and nano rods or tubes through nonlocal Euler–Bernoulli and Timoshenko beam theories. They derived explicit solutions for the static deformation of such structures with standard boundary conditions.

The dynamic properties of the beams using the NLE model were investigated by Lu et al. (2006). They established a nonlocal Euler–Bernoulli beam model based on this theory and presented the frequency equations and shape modes of the beam structures with some typical boundary conditions based on the derived model.

Thai (2012) presented a nonlocal beam theory to analyze bending, buckling, and vibration of the nano beams. He derived the equations of motion from Hamilton's principle and reported analytical solutions for deflection, buckling load, and natural frequency of a simply supported beam. There are also some other papers regarding the application of the NLET to develop various models from the CETs to nonclassical theories, Maachou et al. (2011), Hashemi and Samaei (2011).

In addition, the NLET was applied to study different mechanical behaviors of the carbon nanotubes (CNTs) including their buckling, vibration and instability, as well; Arash and Wang (2012), Wang et al. (2012), Kiani (2012). In these papers, the CNT is majorly investigated using the Euler-Bernoulli or Timoshenko beam models. In our previous paper, we studied the static behaviors and pull-in of the electrostatically actuated CNTs; Fakhrabadi (2014a). However, up to our knowledge, this theory has not been applied to study the dynamic electrostatic actuations of the CNTs. Thus, in this paper, we are going to investigate the dynamic behavior and dynamic pull-in instability of the CNTs using the NLET.

2   DEFINITION OF THE PROBLEM AND MATHEMATICAL FORMULATION

This section provides the definition of the problem under consideration and its governing equations. As shown in Fig. 1, a single-walled CNT is suspended over some graphene sheets with an initial gap equaling G_0 (state 1 in the figure). The CNT as the positive electrode and graphene sheets as the negative electrode (ground plate) are applied an electrical potential difference (V). The charge distributions over the electrodes make an attractive force between the positive and negative electrodes. This force cooperated with the interatomic force between the electrodes leads to deflect the CNT towards the ground plate (state 2 in Fig. 1). The deflection value ($w = w(x)$ in Fig. 1) is proportional to the applied voltage up to where the elastic force of the CNT cannot tolerate the attractive force resulted from the applied voltage and interatomic forces, anymore. In this case, its tip for the cantilevered CNT or its center point for the doubly clamped CNT suddenly drops on the ground plate. This phenomenon is called pull-in instability and the corresponding voltage is pull-in voltage.

Depending on the static or dynamic instability of the CNT, the pull-in phenomenon is called static or dynamic. This paper focuses on the dynamic pull-in of the CNT.
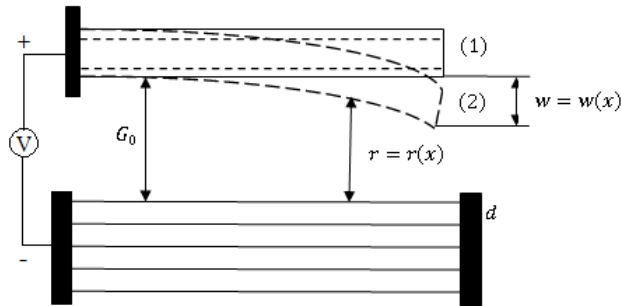

Figure 1: Schematic representation of the cantilevered CNT deflection under electrostatic actuation.

As mentioned before, according to the NLET, the stress at a reference point x in an elastic body not only is a function of the strain at the point but also relates to the strain in whole volume of the elastic boy. Disregarding the body forces, the basic equations for a linear homogenous and isotropic elastic solid is as below, Arash and Wang (2012):

$$\sigma_{ij,j} = 0 \tag{1}$$

$$\sigma_{ij}(x) = \int \lambda\left(\left|x - x^*\right|, \alpha\right) C_{ijkl} \epsilon_{kl}\left(x^*\right) d\Omega\left(x^*\right), \qquad \forall x \in \Omega \tag{2}$$

$$\varepsilon_{ij} = \frac{1}{2}\left(u_{i,j} + u_{j,i}\right) \tag{3}$$

where σ_{ij} and ε_{ij} respectively denote the stress and strain tensors. In additions, C_{ijkl} and u_i are the elastic modulus tensor in classical elasticity and the displacement vector, respectively. Eqs. (1-3) reveal that the stress in a certain point, $\sigma_{ij}(x)$, depends on the local strain at the point x^* resulted from the deformation within a finite volume Ω surrounding the material point, by means of a nonlocal kernel, $\lambda\left(\left|x - x^*\right|, \alpha\right)$, weighing the classical strain around the point x. Moreover, λ is known as the nonlocal modulus or attenuation factor that is a function of the distance between the points, $\left|x - x^*\right|$, as well as the material constant α. The latter defined as $e_0 a / l$ where a is the internal characteristics length such as lattice constant, granular size or distance between the C-C bonds, l is the external characteristics length such as the crack length or wave length and e_0 is a material-dependant constant. So far, there is no rigorous study made on estimating the scale coefficient and due to dependency of the small-scale parameter on the size and chirality of the CNT, most of the researches conducted on the effects of nonlocal elasticity on mechanical behaviors of the CNTs studied a range of various values. Eringern suggested that the kernel function can be defines as below, Arash and Wang (2012):

$$\lambda\left(\left|x\right|, \alpha\right) = \frac{1}{2\pi l^2 \alpha^2} K_0\left(\frac{\sqrt{x\,x}}{l\alpha}\right) \tag{4}$$

where K_0 is the modified Bessel's function. Replacing Eq. (4) into Eq. (2), the constitutive equation governing the elastic behavior of the linear homogeneous and isotropic material is obtained as below:

$$\left(1-\left(e_0 a\right)^2 \nabla^2\right)\sigma = C : \varepsilon \tag{5}$$

where ∇^2 is the Laplacian operator. The Euler-Bernoulli beam has been used in different studies as a model to investigate the mechanical behaviors of the CNTs. In this paper, we also apply it in order to investigate the dynamic electromechanical properties of the CNTs under electrostatic actuation. In this model, the Hook's law for the one-dimensional stress state is presented as below:

$$\sigma(x) - \left(e_0 a\right)^2 \frac{\partial^2 \sigma(x)}{\partial x^2} = E\,\varepsilon(x) \tag{6}$$

where E is the elastic modulus of the body and x is the coordinate along the length of the CNT. According to the concepts of elasticity, the resultant bending moment, M, and axial strain, $\varepsilon(x)$, in the CNT, can be obtained from Eqs. (7a) and (7b).

$$M = \int_A z\,\sigma\,dA \tag{7a}$$

$$\varepsilon_x = -z\,\frac{\partial^2 w}{\partial x^2} \tag{7b}$$

where z is the coordinate measured from the mid-plane in the radius direction of the CNT, $w(x,t)$ is the transverse deflection and A is the cross-sectional area of the CNT.

The governing equation to the vibration of the CNT applied an axial load, N, and transverse distributive force, q, can be formulated as below:

$$\frac{\partial Q}{\partial x} = m_c\,\frac{\partial^2 w}{\partial t^2} + c\,\frac{\partial w}{\partial t} + q(x) \tag{8a}$$

$$Q - \frac{\partial M}{\partial x} + N\,\frac{\partial w}{\partial x} = 0 \tag{8b}$$

where $Q(x,t)$ is the shear force applied on the CNT. In addition, m_c and c are respectively the mass of the CNT per unit length and damping coefficient. In order to calculate m_c, the number of carbon atoms for a given chirality and length is calculated. This number is multiplied by the mass of the carbon atom yields the total mass of the CNT. The continuum model of the CNT is a beam with hollow circular cross section (with given diameter, thickness and length). The total mass of the CNT divided by the area of the mentioned model yields the mass per unit length. Substituting Eq. (8b) into Eq. (8a) results in the vibration equation of the CNTs using the NLET presented in Eq. (9).

$$EI \frac{\partial^4 w}{\partial x^4} - N \frac{\partial^2}{\partial x^2}\left(w - (e_0 a)^2 \frac{\partial^2 w}{\partial x^2}\right) + m_c \frac{\partial^2}{\partial t^2}\left(w - (e_0 a)^2 \frac{\partial^2 w}{\partial x^2}\right) + c \frac{\partial}{\partial t}\left(w - (e_0 a)^2 \frac{\partial^2 w}{\partial x^2}\right) = q(x) - (e_0 a)^2 \frac{\partial^2 q(x)}{\partial x^2} \quad (9)$$

where I and t are the moment of inertia and time, respectively. The axial force is considered the mid-plane stretching effects for the doubly clamed CNTs and is supposed zero for the cantilevered ones. The above equation was obtained for straight CNTs. For the CNTs with larger aspect ratios, waviness plays important roles. However, in this paper, we focus only on the CNTs with negligible waviness. Thus, Eq. (9) can be rewritten for the doubly clamped CNTs as Eq. (10a):

$$EI \frac{\partial^4 w}{\partial x^4} - \left(\frac{EA}{2L} \int_0^L \left(\frac{\partial w}{\partial x}\right)^2 dx\right) \frac{\partial^2}{\partial x^2}\left(w - (e_0 a)^2 \frac{\partial^2 w}{\partial x^2}\right) + m_c \frac{\partial^2}{\partial t^2}\left(w - (e_0 a)^2 \frac{\partial^2 w}{\partial x^2}\right)$$

$$(10a)$$

$$+ c \frac{\partial}{\partial t}\left(w - (e_0 a)^2 \frac{\partial^2 w}{\partial x^2}\right) = q(x) - (e_0 a)^2 \frac{\partial^2 q(x)}{\partial x^2}$$

Subjected to the following boundary conditions:

$$\frac{\partial w(0,t)}{\partial x} = w(0,t) = \frac{\partial w(L,t)}{\partial x} = w(L,t) = 0 \quad (10b)$$

On the other hand, disregarding the von Karman nonlinearity for the cantilever boundary conditions, the resultant equation governing the vibration of the cantilevered CNTs is as below:

$$EI \frac{\partial^4 w}{\partial x^4} + m_c \frac{\partial^2}{\partial t^2}\left(w - (e_0 a)^2 \frac{\partial^2 w}{\partial x^2}\right) + c \frac{\partial}{\partial t}\left(w - (e_0 a)^2 \frac{\partial^2 w}{\partial x^2}\right) = q(x) - (e_0 a)^2 \frac{\partial^2 q(x)}{\partial x^2} \quad (11a)$$

Subjected to the following boundary conditions:

$$\frac{\partial w(0,t)}{\partial x} = w(0,t) = 0$$

$$(11b)$$

$$EI \frac{\partial^2 w(L,t)}{\partial x^2} - (e_0 a)^2 q(x) = EI \frac{\partial^3 w(L,t)}{\partial x^3} - (e_0 a)^2 \frac{\partial q(x)}{\partial x} = 0$$

The distributed force $q(x)$ in Eqs. (10a) and (11a) composes of electrostatic and vdW components. The electrostatic force adopted from Dequenses (2002) and adapted for our problem is presented as:

$$q_{elec} = \frac{\pi \varepsilon_0 V^2}{\sqrt{(G_0 - w)(G_0 - w + 2R)} \, \text{arccosh}^2\left(1 + \frac{G_0 - w}{R}\right)} \quad (12)$$

where ε_0, V, R and G_0 respectively represent electrical permittivity, voltage, radius of the CNT and initial gap.

In addition, vdW force is calculated from the formula presented in Dequesnes et al. (2002) after some variable changes and computational effort:

$$q_{vdw} = \frac{\pi^2 c_6 \sigma^2}{2} \sum_{n=1}^{N_G} \frac{R \left(\begin{array}{c} 8\left(G_0 + (n-1)d - w\right)^4 + 32\left(G_0 + (n-1)d - w\right)^3 R \\ +72\left(G_0 + (n-1)d - w\right)^2 R^2 + 80\left(G_0 + (n-1)d - w\right)R^3 + 35R^4 \end{array} \right)}{\left(G_0 + (n-1)d - w\right)^{\frac{9}{2}} \left(G_0 + (n-1)d - w + 2R\right)^{\frac{9}{2}}} \tag{13}$$

where c_6 and σ^2 are Lennard-Jones potential parameters describing vdW force and N_G represents the number of graphene sheets. The following lines belong to the numerical approaches applied to solve the above governing equations.

2.2 Solution of the Governing Equations

Applying the following nondimensional parameters, one can nondimesionalize the terms of Eqs. (10)- (13).

$$\bar{w} = \frac{w}{G_0}, \bar{x} = \frac{x}{L}, \bar{R} = \frac{R}{G_0}, \bar{d} = \frac{d}{G_0}, \bar{t} = \frac{t}{t^* = \sqrt{\frac{m_c L^4}{EI}}} \tag{14}$$

In this paper, it is assumed that there is not any external axial force on the systems, i. e. $N=0$. Substituting the above nondimensional variables in Eqs. (10a) and (11a) results in:

$$\frac{\partial^4 \bar{w}}{\partial \bar{x}^4} - \alpha_1 \frac{\partial^2 \bar{w}}{\partial \bar{x}^2} + \alpha_{1NL} \frac{\partial^4 \bar{w}}{\partial \bar{x}^4} + \beta_1 \frac{\partial^2 \bar{w}}{\partial \bar{t}^2} - \beta_{1NL} \frac{\partial^4 \bar{w}}{\partial \bar{t}^2 \partial \bar{x}^2} + \gamma_1 \frac{\partial \bar{w}}{\partial \bar{t}} - \gamma_{1NL} \frac{\partial^3 \bar{w}}{\partial \bar{t} \partial \bar{x}^2} \tag{15}$$
$$= \bar{q}_{elec} + \bar{q}_{vdW} - e_{NL}^2 \frac{\partial^2 (\bar{q}_{elec} + \bar{q}_{vdW})}{\partial \bar{x}^2}$$

where,

$$\alpha_1 = \left[\left(\alpha \int_0^1 \left(\frac{d\bar{w}}{d\bar{x}} \right)^2 d\bar{x} \right) \right]$$

$\alpha = \frac{A G_0^2}{2I}$ for doubly clamped boundary conditions and $\alpha = 0$ for cantilever boundary conditions

$$\alpha_{1NL} = \left[\left(\alpha_{NL} \int_0^1 \left(\frac{d\bar{w}}{d\bar{x}} \right)^2 d\bar{x} \right) \right] \tag{16}$$

$\alpha_{NL} = \frac{AG_0^2}{2I}(e_{NL})^2$ for doubly clamped boundary conditions and $\alpha_{NL} = 0$ for cantilever boundary conditions.

$$e_{NL} = \frac{e_0 a}{L}$$

$$\beta_1 = m_c \frac{L^4}{EIt^{*2}}$$

$$\beta_{1NL} = m_c \frac{L^4}{EIt^{*2}} \left(e_{NL}\right)^2$$

$$\gamma_1 = \frac{cL^4}{EIt^*}$$

$$\gamma_{1NL} = \frac{cL^4}{EIt^*} \left(e_{NL}\right)^2$$

$$\beta = \frac{\pi\varepsilon_0 L^4}{EIG_0^2}$$

$$\bar{q}_{elec} = \frac{\beta V^2}{\sqrt{(1-\bar{w})(1-\bar{w}+2\bar{R})}\,\text{arccosh}^2\left(1+\dfrac{1-\bar{w}}{\bar{R}}\right)}$$

$$\gamma = \frac{\pi^2 c_6 \sigma^2 L^4}{2EIG_0^5}$$

$$\bar{q}_{vdW} = \gamma \sum_{n=1}^{N_G} \frac{\bar{R}\left(\begin{array}{c} 8\left(1+(n-1)\bar{d}-\bar{w}\right)^4 + 32\left(1+(n-1)\bar{d}-\bar{w}\right)^3\bar{R} \\ +72\left(1+(n-1)\bar{d}-\bar{w}\right)^2\bar{R}^2 + 80\left(1+(n-1)\bar{d}-\bar{w}\right)\bar{R}^3 + 35\bar{R}^4 \end{array}\right)}{\left(1+(n-1)\bar{d}-\bar{w}\right)^{\frac{9}{2}}\left(1+(n-1)\bar{d}-\bar{w}+2\bar{R}\right)^{\frac{9}{2}}}$$

In order to solve the governing equation of the dynamic behavior of the CNT under electrostatic actuation, the expansion theory is applied for Eq. (15) as following, Nayfeh et al. (2007):

$$\psi(x) = \sum_{j=1}^{N} T_j(t)\varphi_j(x) \tag{17}$$

The shape modes, $\varphi_j(x)$, corresponding to the cantilever and doubly clamped boundary conditions are presented in Eqs. (18) and (19), respectively.

$$\varphi(x) = \cosh\mu_{sm}\bar{x} - \cos\mu_{sm}\bar{x} - \frac{(\cosh\mu_{sm} + \cos\mu_{sm})}{(\sinh\mu_{sm} + \sin\mu_{sm})}(\sinh\mu_{sm}\bar{x} - \sin\mu_{sm}\bar{x}), \tag{18}$$
$$\mu_{sm1} = 1.875$$

$$\varphi(x) = \cosh\lambda_{sm}\bar{x} - \cos\lambda_{sm}\bar{x} - \frac{(\cosh\lambda_{sm} - \cos\lambda_{sm})}{(\sinh\lambda_{sm} - \sin\lambda_{sm})}(\sinh\lambda_{sm}\bar{x} - \sin\lambda_{sm}\bar{x}), \tag{19}$$
$$\lambda_{sm1} = 4.73$$

Replacing the first term of Eq. (17) in Eq. (15) results in Eq. (20):

$$T(1 + \alpha_{1NL})\frac{d^4\varphi}{d\bar{x}^4} - \alpha_1 T\varphi + \beta_1 \ddot{T}\varphi - \beta_{1NL}\ddot{T}\varphi + \gamma_1 \dot{T}\varphi - \gamma_{1NL}\dot{T}\varphi$$
$$= \bar{q}_{elec} + \bar{q}_{vdW} - e_{NL}^2 \frac{\partial^2(\bar{q}_{elec} + \bar{q}_{vdW})}{\partial \bar{x}^2} \tag{20}$$

Applying Galerkin method to the above equation, we have:

$$T(\underset{1}{k_{1d}} - \alpha_1 k_{2d}) + \dot{T}(\gamma_1 \underset{1}{k_{3d}} - \gamma_1 k_{3dNL}) + \ddot{T}(\beta_1 \underset{1}{k_{4d}} - \beta_{1NL}k_{4dNL}) \tag{21}$$
$$= \int_0^1 \bar{q}_{elec}\varphi d\bar{x} + \int_0^1 \bar{q}_{vdW}\,\varphi d\bar{x} - \int_0^1 e_{NL}^2 \frac{\partial^2(\bar{q}_{elec} + \bar{q}_{vdW})}{\partial \bar{x}^2}\varphi d\bar{x}$$

where

$$k_{1d} = (1 + \alpha_{1NL})\int_0^1 \frac{d^4\varphi}{d\bar{x}^4}\varphi d\bar{x}$$

$$k_{2d} = k_{3dNL} = k_{4dNL} = \int_0^1 \frac{d^2\varphi}{d\bar{x}^2}\varphi d\bar{x} \tag{22}$$

$$k_{3d} = k_{4d} = \int_0^1 \varphi^2 d\bar{x}$$

Eq. (21) is solved using the 4th order Runge-Kutta method in order to analyze the dynamic behaviors of the system. It is worth noting that the static deflection of the CNT under the vdW interaction before applying the DC voltage is calculated using step by step linearization method, Rezazadeh et al. (2006), Fakhrabadi et al. (2014).

3 RESULTS AND DISCUSSION

In this section, the results obtained from the formulations are presented and compared with those calculated using the CET. The numerical values used in the paper are presented in table 1. The initial parameters denoting with an asterisk were adopted from Dequesnes et al. (2002) and the others are assumptions. These data are fixed unless stated explicitly.

Parameters	Numerical values
*Elastic modulus (TPa)	1
Gap distance (nm)	4
*Electric permittivity (F/m)	8.854e-12
Length (nm)	50
Radius (A)	6.785 for chirality (10,10)
*Thickness (A)	3.4
*Lennard-Jones first parameter (c_6) (Nm^7) *	2.43×10^{-78}
*Lennard-Jones first parameter (σ) (m^{-3})	1.14×10^{29}
Nonlocal parameter (e_{NL})	0.2

Table 1: Numerical values applied in the paper.

In our previous studies, we investigated the static pull-in behaviors of the CNTs using molecular dynamics; Fakhrabadi et al (2013), Fakhrabadi et al (2014b), Fakhrabadi et al (2014c). We proved that for a CNT having length 20 nm and chirality (10,10), the pull-in voltage obtained from molecular dynamics is approximately 15% higher than the pull-in voltage estimated by the CET (Fakhrabadi 2013). However, it seems that this value is not fixed and depends on the chirality and length of the nanotube. Thus, in this paper, we apply the NLET in order to scrutinize the effects of a size-dependent behavior using nonclassical theory.

Figures 2 (a)-(d) demonstrate the vibration and phase planes of the cantilevered and doubly clamped CNTs under step DC voltages. The results are presented for both CET (dashed lines) and NLET (solid lines). As explained before, application of voltage to the system results in deflection of the CNT towards the graphene sheets. If the applied voltage is AC or step DC, the deflection will be oscillatory due to the nature of the actuation. As shown in the figures, the CNT represents harmonic motion in case of applying step DC voltage up to a maximum threshold. Below the limit, increasing applied voltage increases the vibration amplitude of the nano system. But, when the applied voltage reaches to the maximum limit, the CNT does not follow the previous harmonic motions, anymore and diverges from them. This phenomenon is called dynamic pull-in corresponding the saddle-node bifurcation. The threshold divergence voltage is known as the snap-down or pull-in voltage.
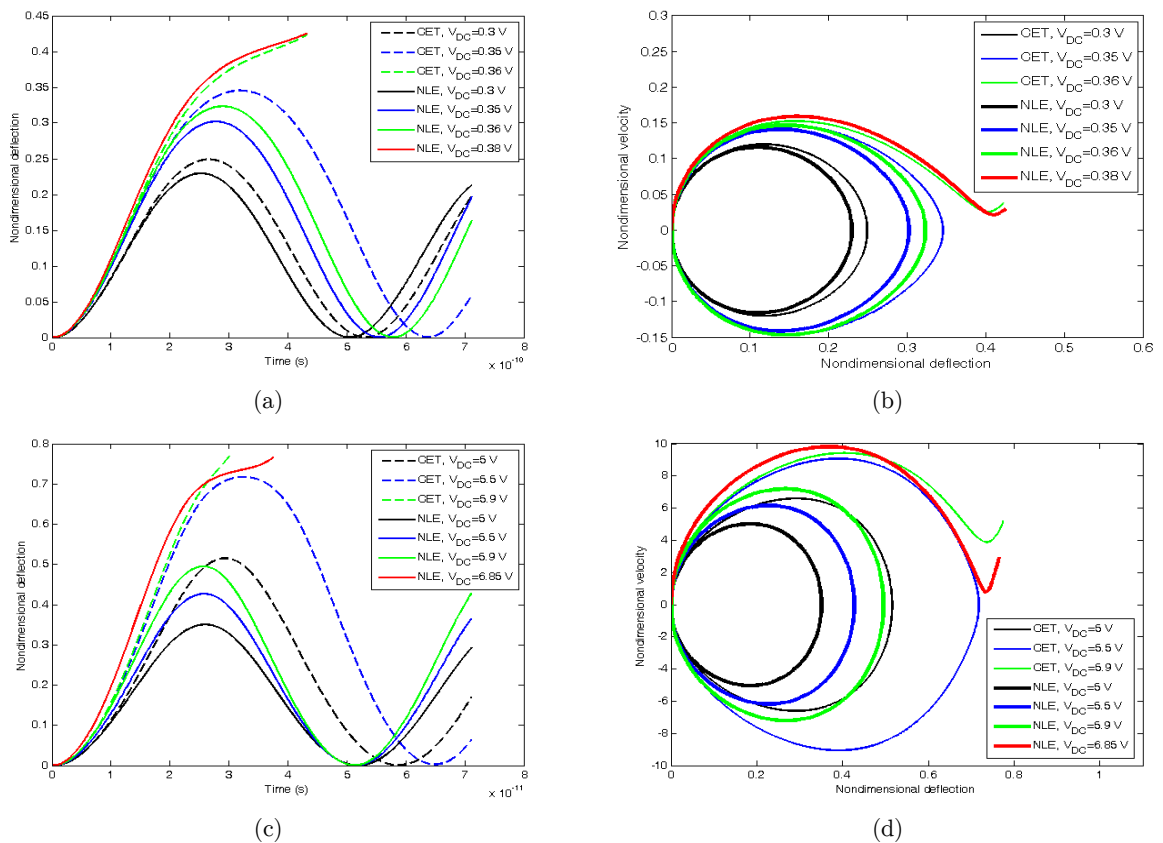

Figure 2: Vibration and phase planes of the CNT with (a) and (b) cantilever, (c) and (d) doubly clamped boundary conditions.

The figures reveal that application of the NLET results in stiffer structures with smaller vibration amplitude in comparison to the outcomes computed via the CET. Since the mechanical behaviors of the CNTs are size-dependent, they can be estimated reliably with the nonclassical theorems such as NLET. Thus, the CET overestimates the vibration amplitudes and consequently, underestimates the dynamic pull-in voltages. For example, the pull-in voltage of the cantilevered CNT is computed 0.36 V using the CET and 0.38 V via application of the NLET. The difference is greatly considerable for the doubly clamped CNTs (5.9 V using the CET and 6.85 V using the NLET).

The one-by-one comparison between the Figs. 2 (a) and (c) and Figs. 2 (b) and (d) prove that the vibration of the doubly clamped CNTs demands higher voltages than the vibration of the cantilevered CNTs, with same dimensions. This matter can be attributed to the stiffer structures of the former due to the type of the boundary conditions as well as the mid-plane stretching effects. Obviously, in case of same dimensions, the pull-in voltages of the doubly clamped CNTs are remarkably larger than the pull-in voltages of the CNTs with the cantilever boundary conditions.

Figures 3 (a) and (b) respectively display the effects of increasing nonlocal parameter on the dynamic pull-in voltages of the CNTs with the cantilever and doubly clamped boundary conditions. According to the figures, increasing nonlocal parameter increases the pull-in voltages of the CNTs with both boundary conditions but the influences are stronger for the doubly clamped CNTs. This can be attributed to additional effects of the application of NLET on the axial force resulted from the mid-plane stretching in the doubly clamped CNTs. The figures reveal that application of the NLET makes significant changes in the mechanical behaviors of the nano structures, in general, and in the pull-in voltages, in particular. Thus, it should be applied in design, modeling and implementation of the NEMS. Otherwise, the simulated systems may deviate from the real ones. The resulted errors between the modeled and implemented systems will propagate in case of integrated application of the CNT-based NEMS such as integrated circuits.
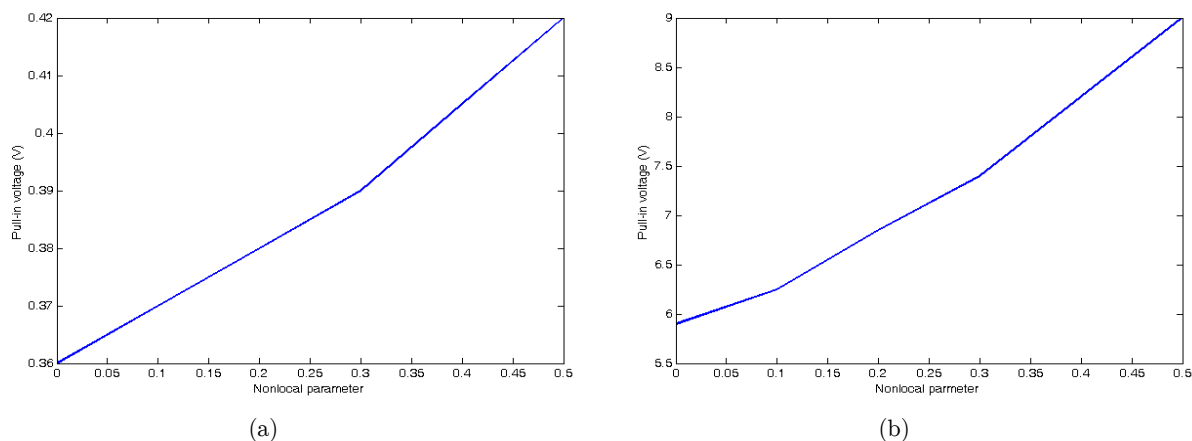

| (a) | (b) |

Figure 3: Pull-in voltages of the (a) cantilevered, (b) doubly clamped CNTs vs. nonlocal parameter.

As mentioned before, one of the main applications of the studied system is in nano resonators. Therefore, estimating exact natural frequencies of the nano system for this application is extremely important. Thus, in Figures 4 (a) and (b), the effects of NLET on the principle natural frequencies of the cantilever and doubly clamped CNTs are investigated. According to the figures, increasing

the actuation voltage decreases the natural frequencies of the CNTs with both boundary conditions. This is because of weakening the stiffness of the nano systems with approaching to the pull-in region. Moreover, increasing nonlocal parameters increases the stiffness and consequently, the natural frequencies of the CNTs. It seems that the gradient of increment increases with increasing the nonlocal parameter.
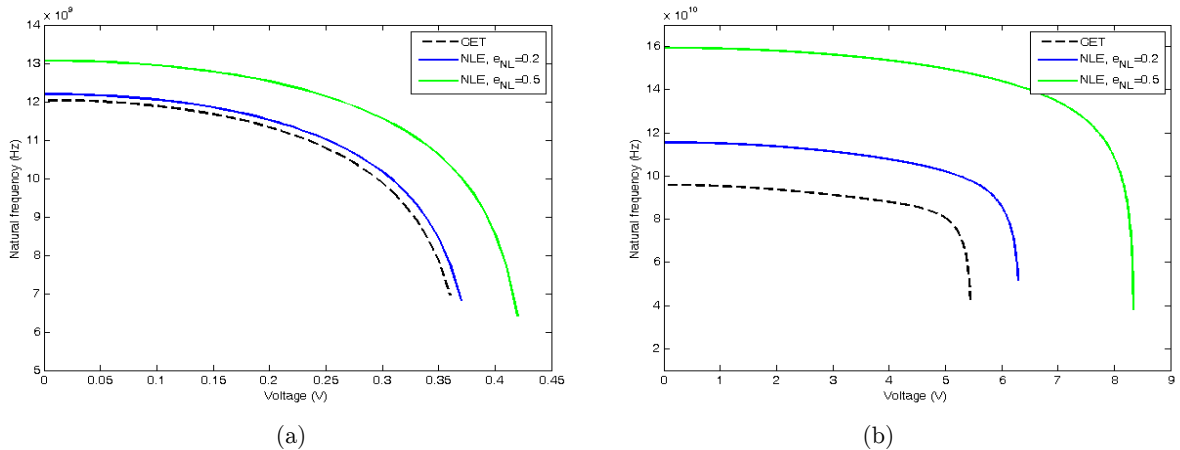

(a)   (b)

Figure 4: Natural frequencies of the (a) cantilevered, (b) doubly clamped CNTs vs. voltage.

Figures 5 (a) and (b) illustrate the effects of length variation on the dynamic pull-in voltages of the CNTs with the cantilever and doubly clamped boundary conditions. The figures reveal that increasing the length decreases the pull-in voltages of the CNTs with both boundary conditions. This matter can be attributed to mechanical weakening of the nano structure with increasing length. The figures show that application of the NLET increases the pull-in voltages and its effects weaken with increasing the length. It seems that the results computed from the CET and NLET approach each other for longer CNTs.
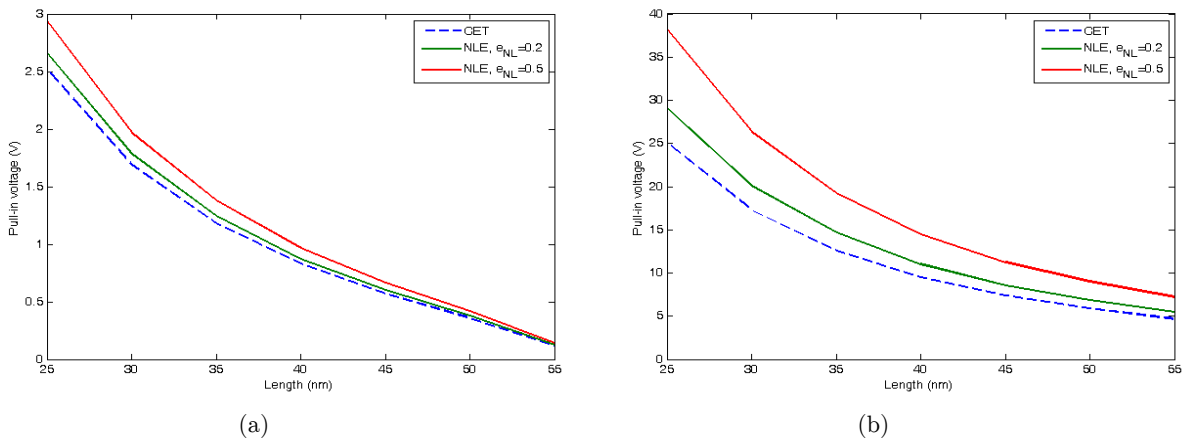

(a)   (b)

Figure 5: Pull-in voltages of the (a) cantilevered, (b) doubly clamped CNTs vs. length.

The effects of changes in the radius of the CNTs with the cantilever and doubly clamped boundary conditions on the dynamic pull-in voltages are displayed in Figures 6 (a) and (b). According to the figures, one may conclude that increasing radius increases the pull-in voltages of the CNTs with both boundary conditions. This fact is due to strengthening the nano structure with increasing the radius. The stiffer structures with larger diameters obviously possess higher pull-in voltages. The figures reveal that the effects of application of NLET increase with increasing the radius.
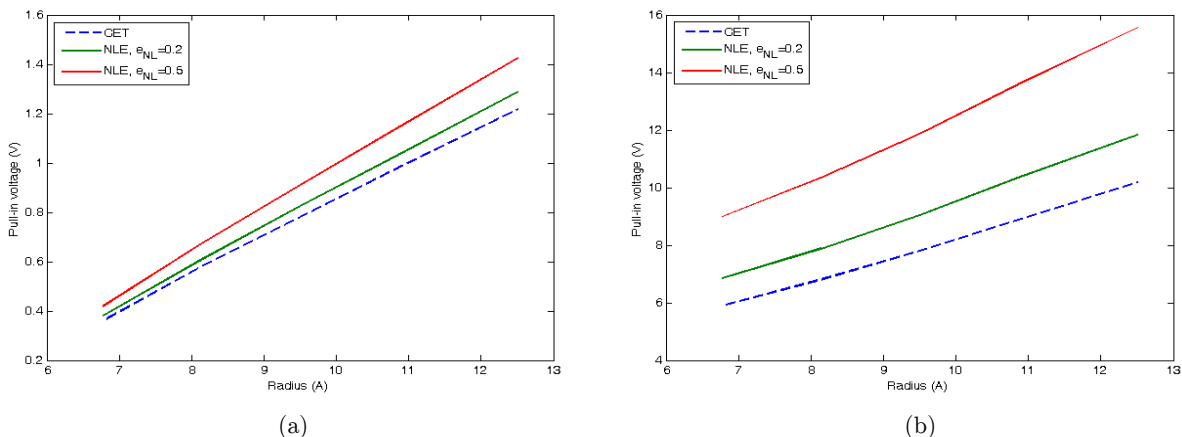

(a)   (b)

Figure 6: Pull-in voltages of the (a) cantilevered, (b) doubly clamped CNTs vs. radius.

Figures 7 (a) and (b) show the influences of increasing gap between the electrodes on the dynamic pull-in voltages of the CNTs with the considered boundary conditions. The figures prove that increasing the gap results in increasing the dynamic pull-in voltages. This matter is due to weakening the effects of electrostatic and vdW forces with increasing the gap because they both are gap-dependent forces and are inversely proportional to its value. Thus higher voltages should be applied to compensate this weakening. In addition, increasing the gap strengthens the effects of the NLET.
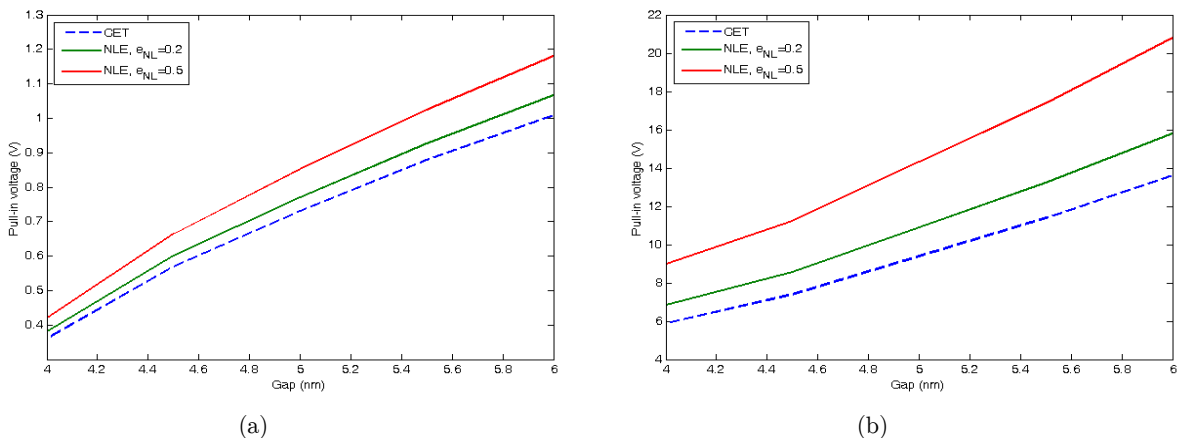

(a)   (b)

Figure 7: Pull-in voltages of the (a) cantilevered, (b) doubly clamped CNTs vs. gap distance.

The results presented above were for the undamped vibration of the CNTs. In the following lines, we are going to investigate the effects of damping on the dynamic pull-in voltages. Figures 8 (a)-(d) depict the damped vibration and phase planes of the CNTs with the cantilever and doubly clamped boundary conditions. The damping ratio is considered 0.1. As expected and shown in the figures, the vibration amplitude damps with the time for smaller voltages. After reaching the maximum value, the CNT does not follow the previous damped oscillatory motion and diverges from it. The main point regarding the damped dynamic pull-in voltages of the CNTs is their higher values in comparison to the undamped pull-in voltages. For example, the undamped pull-in voltages of the cantilevered CNT with the properties mentioned in table 1 computed using the NLET is 0.38 V whereas this value reaches to 0.42 V with application of damping to the system. Similar conclusions can be inferred for the doubly clamped CNTs. Thus, variation of damping can be an appropriate choice to control the dynamic pull-in of the nano system.
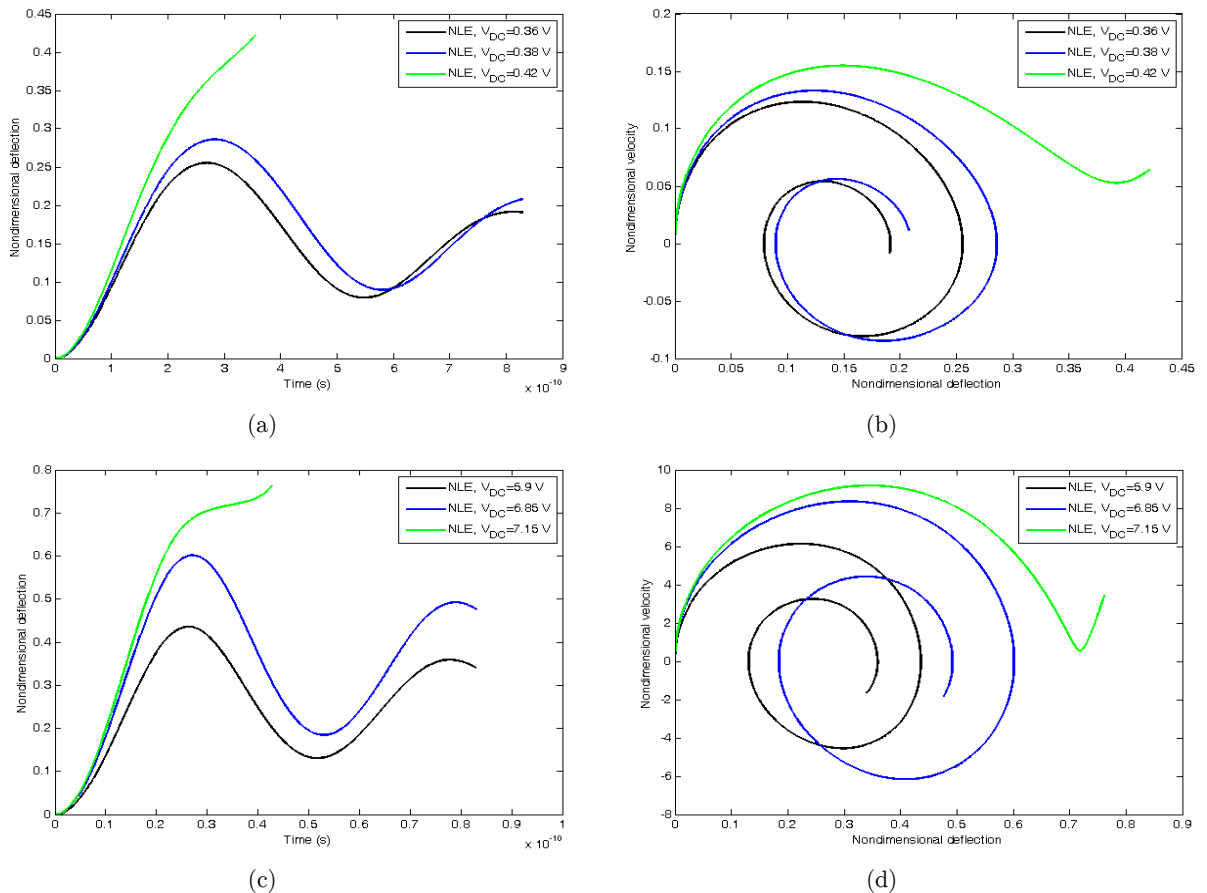

(a)   (b)

(c)   (d)

Figure 8. Vibration and phase plane of the electrostatically actuated CNTs
with (a) and (b) cantilever, (c) and (d) doubly clamped boundary conditions.

Figures 9 (a) and (b) represent the effects of changes in the damping ratios on the dynamic pull-in voltages of the CNTs with the cantilever and doubly clamped boundary conditions. The figures reveal that increasing the damping ratio increases the dynamic pull-in voltages of the CNTs with

both boundary conditions. Similar to the previous cases, application of the NLET leads to the stiffer CNT models with higher pull-in voltages. It seems that the gradient of increment reduces with increasing damping ratio. This fact is more obvious for the cantilevered CNT.
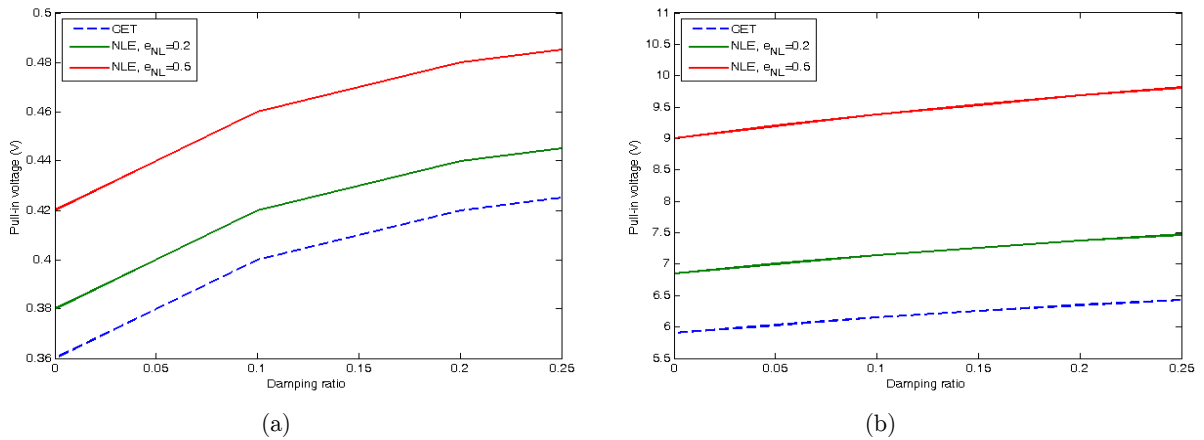

Figure 9: Pull-in voltages of the (a) cantilevered, (b) doubly clamped CNTs vs. damping ratio.

4   CONCLUSION

The paper studied the nonlinear dynamic behaviors of the single-walled CNTs under electrostatic actuation using the NLET and compared the results with those computed from the CET. The effects of changes in length, diameter and gap distance on the dynamic pull-in voltages of the CNTs with the cantilever and doubly clamped boundary conditions were scrutinized. The CNTs with larger diameters and gaps between the electrodes as well as smaller lengths have larger dynamic pull-in voltages. In addition, the results proposed higher dynamic pull-in voltages for the CNTs with the doubly clamped boundary conditions in comparison to the cantilevered CNTs. This fact can be attributed to the stiffer structures of the former due to the type of the boundary conditions and mid-plane stretching effects. The results revealed that application of the NLET resulted in higher pull-in voltages for the CNTs with both boundary conditions. However, the effects were stronger for the doubly clamped CNTs. As an example, for a special case considered in the paper, the dynamic pull-in voltage of the cantilever CNT obtained by CET was 0.36 V and by NLET was 0.38 V. On the other hand, the dynamic pull-in voltage of the CNT with same dimensions but with doubly clamped boundary conditions obtained by CET was 5.9 V and by NLET was 6.85 V. The numbers show the stronger effects of the NLET on the doubly clamped CNTs. In addition, the effects of NLET strengthened with increasing the pull-in voltages for both boundary conditions.

Another thing studied in the paper is the effects of damping on the pull-in voltages. The results proved that damping increased the pull-in voltages. For the damping ratio equaling 0.1, the pull-in voltages of the mentioned cantilever and doubly clamped CNTs estimated by the NLET shifted to 0.42 V and 7.15 V, respectively. However, increasing the damping ratio did not increase the pull-in voltages, linearly. The gradient of the influences decreased for larger ratios.

References

Arash, B., Wang, Q. (2012) A review on the application of nonlocal elastic models in modeling of carbon nanotubes and graphenes, Computational Materials Science 51: 303–313.

Chowdhury, R., Adhikari, S., Mitchell, J. (2009). Vibrating carbon nanotube based bio-sensors, Physica E: Low-dimensional Systems and Nanostructures 42:104–109.

Dequesnes, M., Rotkin, S. V., Aluru, N. R. (2002). Calculation of pull-in voltages for carbon-nanotube-based nanoelectromechanical switches, Nanotechnology 13:120–128.

Eringen, A. C., Edelen, D. G. B. (1972). On nonlocal elasticity, International Journal of Engineering Science 10: 233–248.

Fakhrabadi, M. M. S., Amini, A., Rastgoo, A. (2012). Vibrational properties of two and three junctioned carbon nanotubes, Computational Materials Science: 65, 411–425.

Fakhrabadi, M. M. S., Khani, N., Pedrammehr, S. (2012) Vibrational analysis of single-walled carbon nanocones using molecular mechanics approach, Physica E: Low-dimensional Systems and Nanostructures 44:1162–1168.

Fakhrabadi, M. M. S., Rastgoo, A., Ahmadian, M. T. (2013) On the pull-in instability of double-walled carbon nanotube-based nano electromechanical systems with cross-linked walls, Fullerenes, Nanotubes and Carbon Nanostructures, Appeared Online.

Fakhrabadi, M. M. S., Rastgoo, A., Ahmadian, M. T. (2014) Size-dependent instability of carbon nanotubes under electrostatic actuation using nonlocal elasticity, International Journal of Mechanical Sciences 80: 144–152.

Fakhrabadi, M. M. S., Khorasani, P. K., Rastgoo, A., Ahmadian, M. T. (2014) Molecular dynamics simulation of pull-in phenomena in carbon nanotubes with stone-wales defects, Solid State Communications 157: 38–44.

Fakhrabadi, M. M. S., Rastgoo, A., Ahmadian, M. T. (2014) Pull-In Behaviors of Carbon Nanotubes with Vacancy Defects and Residual Stresses, Journal of Computational and Theoretical Nanoscience 11: 153–159.

Hashemi, S. H., Samaei, A. T. (2011). Buckling analysis of micro/nanoscale plates via nonlocal elasticity theory, Physica E: Low-dimensional Systems and Nanostructures 43:1400–1404.

Iijima, S. (1991). Helical microtubules of graphitic carbon, Nature 354: 56–58.

Kananipour, H., Ahmadi, M., Chavoshi, H. (2013). Application of nonlocal elasticity and DQM to dynamic analysis of curved nanobeams, Latin American Journal of Solids and Structures 11:848–853.

Ke, C., Espinosa, H. D. (2005). Numerical analysis of nanotube-based NEMS devices—Part I: Electrostatic charge distribution on multiwalled nanotubes, Journal of Applied Mechanics 72:721–725.

Ke, C., Espinosa, H. D., Pugno, N. (2005). Numerical analysis of nanotube based NEMS devices—Part II: Role of finite kinematics, stretching and charge concentrations," Journal of Applied Mechanics 72:726–731.

Kiani, K. (2013). Vibration analysis of elastically restrained double-walled carbon nanotubes on elastic foundation subjected to axial load using nonlocal shear deformable beam theories International Journal of Mechanical Sciences 68:16–34.

Kiani, K. (2010). A meshless approach for free transverse vibration of embedded single-walled nanotubes with arbitrary boundary conditions accounting for nonlocal effect, International Journal of Mechanical Sciences 52:1343–1356.

Koochi, A., Fazli, N., Rach, R., Abadyan, M. (2014). Modeling the pull-in instability of the CNT-based probe/actuator under the Coulomb force and the van der Waals attraction, Latin American Journal of Solids & Structures 11: 1315–1328.

Lu, P., Lee, H. P., Lu, C., Zhang, P. Q. (2006). Dynamic properties of flexural beams using a nonlocal elasticity model, Journal of applied physics 99:073510.

Maachou, M., Zidour, M., Baghdadi, H., Ziane, N., Tounsi, A. (2011). A nonlocal Levinson beam model for free vibration analysis of zigzag single-walled carbon nanotubes including thermal effects, Solid State Communications 151, 1467–1471.

Nayfeh, A. H., Younis, M. I., Abdel-Rahman, E. M. (2007). Dynamic pull-in phenomenon in MEMS resonators, Nonlinear Dynamics 48:153–163.

Ouakad, H. M., Younis, M. I. (2010). Nonlinear dynamics of electrically actuated carbon nanotube resonators, Journal of computational and nonlinear dynamics 5: 011009.

Rasekh, M., Khadem, S. E., Tatari, M. (2010). Nonlinear behaviour of electrostatically actuated carbon nanotube-based devices, Journal of Physics D: Applied Physics 43:315301.

Rasekh M., Khadem, S. E. (2011). Pull-in analysis of an electrostatically actuated nano-cantilever beam with nonlinearity in curvature and inertia, International Journal of Mechanical Sciences: 53: 108–115.

Rezazadeh, G., Tahmasebi, A., Zubstov, M. (2006). Application of piezoelectric layers in electrostatic MEM actuators: controlling of pull-in voltage, Microsystem technologies, 12:1163–1170.

Scarpa F., Adhikari, S. (2008). Uncertainty modeling of carbon nanotube terahertz oscillators, Journal of Non-Crystalline Solids 354:4151–4156.

Sedighi, H. M. M., Changizian, Noghrehabadi, A. (2013). Dynamic pull-in instability of geometrically nonlinear actuated micro-beams based on the modified couple stress theory, Latin American Journal of Solids and Structures 11: 810–825.

Thai, H. T. (2012). A nonlocal beam theory for bending, buckling, and vibration of nanobeams, International Journal of Engineering Science 52:56–64.

Wang, C. Y., Zhang, J., Fei, Y. Q., Murmu, T. (2012). Circumferential nonlocal effect on vibrating nanotubules, International Journal of Mechanical Sciences, 58:86–90.

Wang, Q. Liew, K. M. (2007). Application of nonlocal continuum mechanics to static analysis of micro-and nano-structures, Physics Letters A 363:236–242.

Yang Y., Lim, C. W. (2012). Non-classical stiffness strengthening size effects for free vibration of a nonlocal nanostructure, International Journal of Mechanical Sciences 54: 57–68.